

# Consideration of dipole orientation angles yields accurate rate equations for energy transfer in the rapid diffusion limit

Joseph V. Mersol,<sup>\*‡</sup> Hailin Wang,<sup>\*‡</sup> Ari Gafni,<sup>†§</sup> and Duncan G. Steel<sup>\*‡</sup>

<sup>\*</sup>Departments of Physics and Electrical Engineering, <sup>†</sup>Institute of Gerontology, and <sup>§</sup>Department of Biological Chemistry, University of Michigan, Ann Arbor, Michigan 48109 USA

**ABSTRACT** Dipole–dipole energy transfer between suitable donor and acceptor chromophores is an important luminescence quenching mechanism and has been shown to be useful for distance determination at the molecular level. In the rapid diffusion limit, where the excited-state lifetime of the donor is long enough to allow the donor and acceptor to diffuse many times their average separation before deexcitation, it is usually assumed that the relative dipolar orientation is completely averaged due to rotational Brownian motion. Under this simplifying assumption, analytical expressions have been derived earlier for the energy transfer rate between donor and acceptor characterized by different geometries. Most such expressions, however, are only approximate because complete angular averaging is permitted only in a geometry that possesses spherical symmetry surrounding each chromophore. In this paper analytical expressions that correctly account for incomplete angle averaging due to steric hindrance are presented for several geometries. Each of the equations reveals a dependence of the energy transfer rate on chromophore orientation. It is shown that correctly accounting for this effect can lead to improvements in estimates of the distance of closest approach from measured quenching rates based on energy transfer experiments.

## INTRODUCTION

Energy transfer from a donor chromophore to an acceptor chromophore by resonance dipole–dipole (Förster) coupling is a significant quenching mechanism of donor luminescence. Because of the strong dependence of the energy transfer rate on the donor–acceptor separation, energy transfer is widely used as a technique for distance measurement at the molecular level and has been applied to the study of protein structure (1–5). The rate of energy transfer also depends on the relative orientations of transition dipole moments of the donor and acceptor, a dependence that substantially complicates the derivation of the energy transfer rate equation. To simplify the analysis it is often assumed that rotational Brownian motion will average out the angular dependence, allowing its replacement with a constant multiplicative factor. This assumption appears especially applicable in the study of energy transfer in the rapid diffusion limit, where the donor excited-state lifetime is long enough to allow the donor and acceptor to translationally diffuse many times their average separation before deexcitation. At small donor–acceptor separations in this limit, however, steric hindrance prevents complete angular averaging for chromophores that are not in a spherically symmetric environment. In this paper we derive the exact form of the energy transfer rate equations in the rapid diffusion limit for several previously considered geometries that lack spherical symmetry, accounting for steric hindrance and

demonstrating the importance of the effects of incomplete angle averaging.

The explicit form of the rate constant  $k_t$  for energy transfer from a donor to an acceptor at a fixed separation distance  $r$  is given by (6)

$$k_t = k_0 \left( \frac{R_0}{r} \right)^6, \quad (1)$$

where  $k_0$  is the decay rate of the donor in the absence of transfer.  $R_0$  has the physical interpretation of being that particular separation where the energy transfer rate equals the deexcitation rate in the absence of transfer, and is given by the expression  $R_0 = 9.79 \times 10^3 (J\kappa^2 Q_0 n^{-4})^{1/6} \text{ \AA}$ .  $Q_0$  is the quantum yield of the donor in the absence of acceptor, and  $n$  is the refractive index of the medium.  $J$  is the spectral overlap integral (in  $\text{cm}^3/\text{M}$ ), given by  $\int f(\lambda) \epsilon(\lambda) \lambda^4 d\lambda / \int f(\lambda) d\lambda$ , where  $f(\lambda)$  is the emission intensity of the donor and  $\epsilon(\lambda)$  is the molar extinction coefficient of the acceptor at wavelength  $\lambda$ .  $\kappa^2$ , the orientation factor, accounts for the relative orientations of the transition dipole vectors and is given by the expression  $\kappa^2 = (\cos \theta_{12} - 3 \cos \theta_1 \cos \theta_2)^2$ , where  $\theta_{12}$  is the angle between the dipole vectors and  $\theta_1$  ( $\theta_2$ ) is the angle between dipole 1 (dipole 2) and the line joining the dipoles. A change in the measured energy transfer rate between a given donor–acceptor pair can thus be due to changes in any of these quantities. Because  $J$ ,  $Q_0$ , and  $n$  can be determined independently, it is clear that

the quenching rate and donor-acceptor separation are uniquely related if  $\kappa^2$  can be determined.

The evaluation of  $\kappa^2$  in geometries with fixed donor-acceptor separation has been the subject of several discussions highlighting the difficulties imposed on distance determination through uncertainties in the values of this parameter. When there is complete rotational freedom of donor and acceptor at the separation distance being considered, then  $\kappa^2$  is equal to  $\frac{2}{3}$  (6). In situations where rotational motion is hindered, however, the evaluation of this quantity may be more complicated.  $\kappa^2$  has previously been considered when there is complete restriction of rotational Brownian motion (7). Other studies have focused on the value of  $\kappa^2$  when there are multiple donors and acceptors, and when the donor rotation is confined to a cone (8). When  $\kappa^2$  is not known explicitly, it is often possible to set limits on its possible range and still extract useful information (5, 9, 10).

When the donor and acceptor are located in different solute molecules, energy transfer is enhanced by translational diffusion. This enhancement is maximal in the rapid diffusion limit, where the average combined distance traversed by donor and acceptor before the donor's decay is much greater than the average donor-acceptor separation distance. This limit is reached when  $6D\tau \gg s^2$ , where  $D$  is the sum of the donor and acceptor diffusion coefficients,  $s$  is the average donor-acceptor separation, and  $\tau$  is the donor excited-state lifetime (11). In this case all donors in a given sample are affected by the same uniform distribution of acceptors and the transfer rate is found by averaging Eq. 1 over all allowed separations and angular orientations of the transition dipoles and multiplying by the number of acceptors  $N_A$ . The transfer rate is then given by

$$k_t = \frac{1}{V_D} \rho_A \int dV_D \int k_0 \left\langle \left( \frac{R_0}{r} \right)^6 \right\rangle_\Omega dV_A. \quad (2)$$

Here the integration is performed over the volume available to the acceptor and donor molecules  $V_A$  and  $V_D$ , and  $\rho_A$  is the density of acceptors, given by  $\rho_A = N_A/V_A$ . For a system in which the acceptors are confined to a planar surface (such as a membrane), the integration is performed over the surface of the plane and  $\rho_A$  is replaced by  $\sigma_A$ , the surface density of acceptors.  $\langle \rangle_\Omega$  represents the angular averaging over the allowed transition dipole orientations of donor and acceptor chromophores. The evaluation of Eq. 2 is difficult because the spatial and angular averages are usually coupled, with the explicit form of the limits of integration depending on the geometry of the model used to represent the molecules involved in the transfer.

One simple model depicts both donor and acceptor as freely diffusing spheres of radii  $r_1$  and  $r_2$ , with each

chromophore located at the spherical center. Due to the complete spherical symmetry around each chromophore in this case, the angular average is independent of the spatial average, allowing complete angular averaging and resulting in the traditional assignment of  $\kappa^2 = \frac{2}{3}$ . Because the chromophores are embedded at the centers of spheres, the lower limit on their separation will be given by  $a = r_1 + r_2$ , where  $a$  is the distance of closest approach, defined as the smallest possible separation between the donor and acceptor chromophores in a given geometry. As shown by Thomas et al. (11), integration of Eq. 2 then yields

$$k_t = \frac{4\pi}{3} k_0 \bar{R}_0^6 \rho_A \frac{1}{a^3}, \quad (3)$$

where for the purpose of this discussion it is convenient to define the variable  $\bar{R}_0$  to be the value of  $R_0$  when  $\kappa^2 = \frac{2}{3}$ ; i.e.,  $\bar{R}_0 = 9.79 \times 10^3 [J(\frac{2}{3}) Q_0 n^{-4}]^{1/6}$ . Because the quenching rate depends on the distance of closest approach between the chromophores, it can be used to determine the radius of either the donor or acceptor sphere if the other radius is known.

In systems lacking spherical symmetry around either chromophore involved in the transfer, the angular and spatial dependences of the energy transfer rate cannot be separately averaged because rotation will be limited for some donor-acceptor separations. Nevertheless, useful approximate analytical transfer rate equations have been developed for several nonspherical systems by assuming that  $\kappa^2$  may be separately averaged, and these have been used to determine distances relevant to the structure of proteins. Yeh and Mearš (12) used a terbium ion as the donor in energy transfer experiments to derive the depth of the iron binding site beneath the surface of human transferrin. Wensel et al. (13) used energy transfer in the rapid diffusion limit to study the interaction of DNA with both intercalating and nonintercalating dye molecules. More recently, Mersol et al. (14) have used the phosphorescent tryptophan residue of *Escherichia coli* alkaline phosphatase as the energy donor to directly determine which of the enzyme's three tryptophans is responsible for its long lived luminescence.

In spite of these and other successful applications, the need to assume that the spatial and angular averages can be separated in the derivation of an analytical solution has represented a significant limitation for further applications of energy transfer in the rapid diffusion limit. Numerical estimates of the effect of the restricted rotation on the relation between the transfer rate and distance have been made for geometries where steric hindrance or binding of a chromophore allows only partial rotation (15, 16), or where one chromophore has

complete rotational and translational freedom while the other is fixed (13, 17).

Initial work in obtaining an analytical solution for the rate of energy transfer in the rapid diffusion limit, without separation of the two averages and thus accounting for restricted rotation, was presented by Kouyama et al. (18) for the simple geometry of Fig. 1. In this geometry a donor molecule is assumed to be embedded a distance  $h$  beneath the surface of a plane (and unable to rotate about any axis parallel to the plane), whereas spherical acceptors of radius  $r$  diffuse freely above the surface of the plane. Careful consideration of the restricted rotation of the donor molecule (using Eq. 2) leads to the following equation for the energy transfer rate (18):

$$k_t = \frac{\pi}{8} \rho_A k_0 \bar{R}_0^6 \frac{1}{(r+h)^3} (1 + \cos^2 \theta_{\mu 1}). \quad (4)$$

Here  $\theta_{\mu 1}$  is the angle between the transition dipole of the membrane-bound chromophore and the line perpendicular to the surface of the plane. This equation shows that there is an explicit dependence of the quenching rate on the orientation of the bound chromophore. If this equation is then averaged over  $\theta_{\mu 1}$  (which physically corresponds to rotating the donor about an axis lying in the plane, thus completing the averaging of  $\kappa^2$ ), then the quenching rate becomes

$$k_t = \frac{4\pi}{3} \rho_A k_0 \bar{R}_0^6 \frac{1}{(r+h)^3} \left(\frac{1}{8}\right), \quad (5)$$

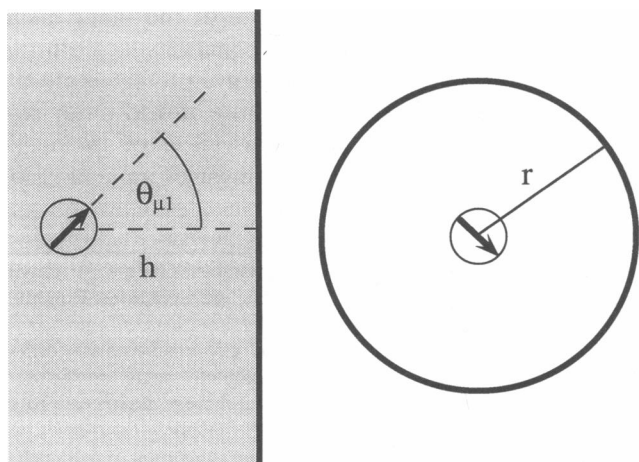


FIGURE 1. The geometry assumed for energy transfer between a freely diffusing acceptor of radius  $r$  and a donor bound in a membrane at a depth  $h$  from the surface. The assumption that  $\kappa^2 = 2/3$  leads to Eq. 5 in the text for the quenching rate, whereas exact accounting for incomplete angular averaging leads to Eq. 4.

which is the same as the equation derived by Stryer et al. (15) under the assumption that  $\kappa^2$  is equal to two-thirds.

## DERIVATION OF RATE EQUATIONS

In this study we extend the calculation of energy transfer rates in the rapid diffusion limit for several geometries without assuming a separation of angular and spatial averages and thereby analytically account for the restricted rotations of embedded chromophores. Fig. 2 summarizes some previously derived approximate formulas and the newly presented exact ones for several geometries. In each of these models the membrane-bound chromophores are assumed to be free to diffuse and rotate in the plane of the membrane only. To obtain the exact transfer rates for these geometries, Eq. 2 was used while explicitly considering the angular average. The derivation is outlined below for the geometry of Fig. 2, row 1, which models a donor and acceptor in spherical molecules of radii  $r_1$  and  $r_2$ , with one chromophore centered and the other off-center by a distance  $t$ . The distance of closest approach here is given by  $a = r_1 + r_2 - t$ . This geometry can be used to represent energy transfer between a donor located off-center in a spherical macromolecule or in the bilayer of a vesicle, while the acceptors are freely diffusing outside.  $\theta_{\mu 1}$ , the angle between transition dipole  $\mu_1$  and the line joining it to the spherical center, is taken to be constant. For this geometry the problem is most easily worked out in the reference frame of the sphere with the off-center chromophore, with the center located at the origin and with the chromophore located at coordinates  $(0, 0, t)$ . The transition dipole associated with this chromophore can be placed in the  $x$ - $z$  plane with unit vector coordinates  $\hat{\mu}_1 = [\sin(\theta_{\mu 1}), 0, \cos(\theta_{\mu 1})]$ , with  $\theta_{\mu 1}$  being fixed. The transition dipole vector of the other chromophore has the unit vector form  $\hat{\mu}_2 = [\sin(\theta_{\mu 2}) \cos(\varphi_{\mu 2}), \sin(\theta_{\mu 2}) \sin(\varphi_{\mu 2}), \cos(\theta_{\mu 2})]$ , and  $\mathbf{r}$  takes the form  $\mathbf{r} = [\rho \sin(\theta_\rho) \cos(\varphi_\rho), \rho \sin(\theta_\rho) \sin(\varphi_\rho), \rho \cos(\theta_\rho) - t]$ . For purposes of calculation it is more convenient to use the vector form of the dipole-dipole interaction terms found in the definition of  $\kappa^2$ , given by  $\cos(\theta_{12}) = \hat{\mu}_1 \cdot \hat{\mu}_2$  and  $3 \cos(\theta_1) \cos(\theta_2) = 3(\hat{\mu}_1 \cdot \hat{r})(\hat{\mu}_2 \cdot \hat{r})$ . Eq. 2 then becomes

$$k_t = k_0 \left( \frac{3}{2} \bar{R}_0^6 \right) \rho_A \int_{r_1+r_2}^{\infty} \rho^2 d\rho \int_{-1}^1 d \cos(\theta_\rho) \int_0^{2\pi} d\varphi_\rho \cdot \left[ \frac{1}{4\pi} \int_{-1}^1 d \cos(\theta_{\mu 2}) \int_0^{2\pi} d\varphi_{\mu 2} \cdot \left[ \frac{(\hat{\mu}_1 \cdot \hat{\mu}_2)}{r^3} - \frac{3(\hat{\mu}_1 \cdot \mathbf{r})(\hat{\mu}_2 \cdot \mathbf{r})}{r^5} \right]^2 \right], \quad (6)$$

with

$$\begin{aligned} & \frac{\hat{\mu}_1 \cdot \hat{\mu}_2}{r^3} - \frac{3(\hat{\mu}_1 \cdot \mathbf{r})(\hat{\mu}_2 \cdot \mathbf{r})}{r^5} \\ &= \frac{1}{r^3} [\sin(\theta_{\mu_1}) \sin(\theta_{\mu_2}) \cos(\varphi_{\mu_2}) + \cos(\theta_{\mu_1}) \cos(\theta_{\mu_2})] \\ & \quad - 3 \frac{1}{r^5} \{ [\rho \sin(\theta_{\mu_1}) \sin(\theta_{\mu_2}) \cos(\varphi_{\mu_2}) \\ & \quad + \rho \cos(\theta_{\mu_1}) \cos(\theta_{\mu_2}) - t \cos(\theta_{\mu_1})] \\ & \quad \times [\rho \sin(\theta_{\mu_2}) \sin(\theta_{\mu_1}) \cos(\varphi_{\mu_1}) \cos(\varphi_{\mu_2}) \\ & \quad + \rho \sin(\theta_{\mu_2}) \sin(\theta_{\mu_1}) \sin(\varphi_{\mu_2}) \cos(\varphi_{\mu_1}) \\ & \quad + \rho \cos(\theta_{\mu_2}) \cos(\theta_{\mu_1}) - t \cos(\theta_{\mu_2})] \}. \end{aligned} \quad (7)$$

The distance  $r$  between the chromophores is given by  $r = [\rho^2 + t^2 - 2t\rho \cos(\theta_{\mu_1})]^{1/2}$ . Because the integrand cannot be factored into terms solely dependent on  $\rho$  and solely dependent on the orientation angles, the spatial and angular averaging are not separable. After expansion of the integrand (which reduces to 105 different terms for this geometry, 10 of which will give nonzero contributions after integration), the integrals in Eq. 6 may be evaluated to give the following equation for the quenching rate:

$$\begin{aligned} k_t = \frac{3}{2} \pi k_0 \bar{R}_0^6 \rho_A & \left( \frac{1}{12} \left[ \frac{8a(a+t)(a+2t)}{a^3(a+2t)^3} \right. \right. \\ & \left. \left. + \frac{(1 + \cos^2 \theta_{\mu_1})[a^3 + (a+2t)^3]}{a^3(a+2t)^3} \right] \right. \\ & \left. + \frac{(1 - 3 \cos^2 \theta_{\mu_1})}{24t^2} \left[ \frac{2(a+t)}{a(a+2t)} + \frac{1}{t} \log \left( \frac{a}{a+2t} \right) \right] \right). \end{aligned} \quad (8)^1$$

The quenching rate thus depends on the angle  $\theta_{\mu_1}$ . As expected, averaging this equation over  $\theta_{\mu_1}$  (which physically would correspond to rotation of the chromophore with respect to the embedding molecule) completes the angular averaging in  $\kappa^2$  and produces the same quenching rate equation that is obtained by assuming that  $\kappa^2 = 2/3$ ,

$$k_t = \frac{4\pi}{3} \rho_A k_0 \bar{R}_0^6 a^{-3} \left( 2 - \frac{a}{a+t} \right)^{-3}, \quad (9)$$

as derived by Thomas et al. (11).

Eq. 8 demonstrates that even freely rotating structures will have restricted angular averaging if their embedded chromophores are not centered. The geometric reason behind this is illustrated by Fig. 3, in which the light circle represents a rotation of sphere 1 about its

off-center chromophore by an angle  $\alpha$  at a small chromophore separation  $r$ . A complete rotation of  $2\pi$  radians about this axis is required to average angle  $\theta_1$  at this particular distance  $r$ . Clearly, however, this cannot be accomplished while maintaining this constant dipole separation due to steric hindrance. Hence the exact derivation of the transfer rate requires leaving  $\kappa^2$  in its unaveraged form and explicitly considering the angles throughout the integration as above. It is worthwhile to note that in the limit where  $t \rightarrow 0$ , this geometry reduces to that of two chromophores embedded at the centers of spheres, whose transfer rate is given by Eq. 3, which was derived assuming a separation of spatial and angular averaging. When this limit is applied to Eq. 8, it indeed reduces to Eq. 3, demonstrating that for spherically symmetric geometries the separation of spatial and angular averaging is a valid assumption. The lack of spherical symmetry is also responsible for incomplete angle averaging in planar surfaces such as that in Fig. 1, because this is a special case of the off-centered sphere of Fig. 3 in the limit that  $r_1, t \rightarrow \infty$  and  $(r_1 - t) = h$ . In this limit the quenching rate equation correspondingly becomes the same as Eq. 4, with  $r_2$  replaced by  $r$ . Thus the absence of spherical symmetry in any geometry requires including  $\kappa^2$  in the spatial and angular averaging of Eq. 2.

The second geometry of Fig. 2 models transfer between an acceptor chromophore confined to the membrane of a vesicle while the donor chromophore is freely diffusing in the intravesicular space. The distance from the center of the vesicle to the bound chromophore is taken to be  $b$ , whereas the distance of closest approach,  $a$ , is the distance from the bound chromophore to the center of a diffusing chromophore at the inner membrane surface. The approximate equations for both this geometry and that of row 1 were used to calculate the position of the retinal chromophore in rod outer segment membranes (17). The derivation of the exact quenching rate in this geometry involves an expression

FIGURE 2. A summary of the assumed geometries for energy transfer and the equations used in calculating their transfer rates. Column 1 depicts the geometric model employed. Column 2 lists the equation for quenching, derived assuming that  $\kappa^2 = 2/3$ . Column 3 lists the form of the transfer rate equations when incomplete angle averaging is properly accounted for. The donor chromophore is assumed to be on the left in each of the models depicted in Column 1; however, the analytical expressions in rows 1 and 4 remain valid upon interchange of donor and acceptor.

Upon interchange of the donor and acceptor in row 2, the equations are modified by substitution of the factor  $\rho_A(b-a)^3/3$  for the factor  $\sigma_A b^2$ . Interchange of the donor and acceptor in row 3 takes energy transfer out of the rapid diffusion limit.

\*This equation results from algebraic simplification of Eq. 8 in reference 17.

<sup>1</sup>A more detailed derivation of this and other equations presented in this paper will be published by the University of Michigan in the Ph.D. thesis of J. V. Mersol.

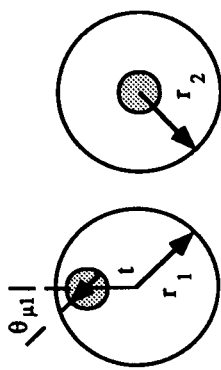
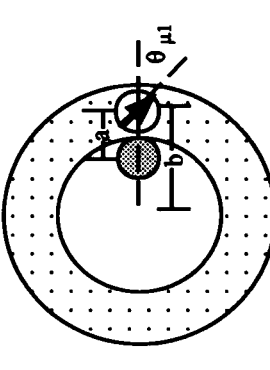
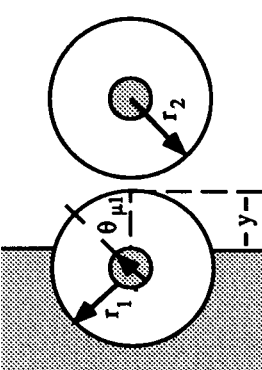
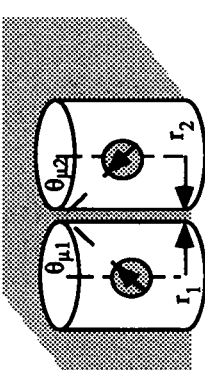
Geometry of transfer	Transfer rate with $\kappa^2=2/3$	Transfer rate with incomplete angle averaging
	$k_t = \frac{4\pi}{3} \rho_A k_o \bar{R}_o^6 a^{-3} \left( 2 - \frac{a}{a+t} \right)^{-3}$ <p>(15) <math>a = r_1 + r_2 - t</math></p>	$k_t = \frac{3\pi}{2} k_o \bar{R}_o^6 \rho_A \left[ \frac{1}{12} \left( \frac{8a(a+t)(a+2t) + (1 + \cos^2 \theta_{\mu 1})(a^3 + (a+2t)^2)}{a^3(a+2t)^3} \right) + \left\{ \frac{(1 - 3\cos^2 \theta_{\mu 1})}{24t^2} \left( \frac{2(a+t)}{a(a+2t)} + \frac{1}{t} \log \left( \frac{a}{a+2t} \right) \right) \right\} \right]$
	$k_t = 4\pi \sigma_A k_o \bar{R}_o^6 \frac{b^2}{a^3} (2b - a)^{-3}$ <p>(17)*</p>	$k_t = 9\pi \sigma_A k_o \bar{R}_o^6 \frac{b^2}{(b-a)^3} \left[ \frac{1}{12b} \left( \frac{1}{(2b-a)^2} - \frac{1}{a^2} \right) + \frac{(1 + \cos^2 \theta_{\mu 1})}{24} \left( \frac{1}{a^3} - \frac{1}{(2b-a)^3} \right) \right] + \left\{ \frac{(1 - 3\cos^2 \theta_{\mu 1})}{48b^2} \left( \frac{1}{a} - \frac{1}{2b-a} \right) + \frac{1}{b} \log \left( \frac{2b-a}{a} \right) \right\} \right]$
	$k_t = \frac{\pi}{2} \rho_A k_o \bar{R}_o^6 \frac{1}{(r_1 + r_2)^3} \left( \frac{1}{3} + \frac{y}{r_1 + r_2} \right)$ <p>(19)</p>	$k_t = \frac{\pi}{2} \rho_A k_o \bar{R}_o^6 \frac{1}{(r_1 + r_2)^3} \left[ \left( \frac{5}{4} - \frac{3}{4} \cos^2 \theta_{\mu 1} \right) \left( \frac{1}{3} + \frac{y}{r_1 + r_2} \right) + (3\cos^2 \theta_{\mu 1} - 1) \frac{(r_1 + r_2)^3 - \frac{1}{2}(r_1 + r_2 - y)^3}{3(r_1 + r_2)^3} \right]$
	$k_t = \frac{\pi}{2} \sigma_A k_o \bar{R}_o^6 \frac{1}{(r_1 + r_2)^4}$ <p>(15)</p>	$k_t = \frac{3\pi}{16} \sigma_A k_o \bar{R}_o^6 \frac{1}{(r_1 + r_2)^4} \left[ 5 \sin^2 \theta_{\mu 1} \sin^2 \theta_{\mu 2} + 4 \cos^2 \theta_{\mu 1} \cos^2 \theta_{\mu 2} \right]$

FIGURE 2

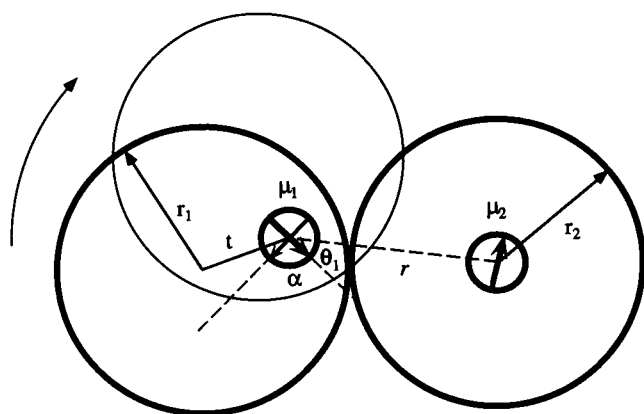


FIGURE 3. An illustration of incomplete angular averaging in diffusion-enhanced energy transfer. Both donor and acceptor are modeled as spheres (shown in bold) of radii  $r_1$  and  $r_2$ , with chromophore  $\mu_2$  at the spherical center and  $\mu_1$  off-center at a distance  $t$ .  $\theta_1$  is the angle between  $\mu_1$  and the line joining it to  $\mu_2$ . The plain circle and arrow represent a rotation of sphere 1 around its off-center chromophore by an angle  $\alpha$ , necessary for averaging  $\theta_1$  at this separation. When  $r$ , the separation between donor and acceptor, is smaller than  $r_1 + r_2 + t$ , any attempt to average the angle  $\theta_1$  by rotating  $\alpha$  through  $2\pi$  radians will be blocked by sphere 2.

very similar to Eq. 6, with the substitution of the appropriate variables  $a$  and  $b$  in the integrand and in  $V_D$ , with the upper and lower limits of the  $\rho$  integration changed to  $(b - a)$  and 0, and with the substitution of  $\rho_A$  for  $\sigma_A$ .

The third geometry of Fig. 2 models transfer between donor and acceptor located at the centers of two spheres of radii  $r_1$  and  $r_2$ , where one sphere is embedded in a plane, extending a distance  $y$  above the planar surface, and where  $\theta_{\mu 1}$  is the angle between the normal to the plane and the transition dipole vector of the embedded chromophore. This is representative of the transfer between a chromophore inside a membrane-bound protein and a chromophore in a freely diffusing spherical molecule. This geometry and its approximate equation were used in energy transfer studies that examined the binding sites of rifamycin and Cibacron blue onto *E. coli* RNA polymerase using Terbium as a donor (19) and are a more generalized geometry compared with that in Fig. 1 used by Kouyama et al. (18).

The final geometry in Fig. 2 models transfer between chromophores at the centers of two cylinders of radii  $r_1$  and  $r_2$ , which are confined to the surface of a membrane with their axes perpendicular to it. The angles between the transition dipoles and the perpendicular to the plane are  $\theta_{\mu 1}$  and  $\theta_{\mu 2}$ . This model represents energy transfer when both chromophores are in a membrane or inside of

membrane-bound proteins. Incomplete angles averaging here is due to the lack of out-of-plane rotation.

As mentioned before, each of the geometries presented in Fig. 2 shows a dependence of the transfer rate of the fixed orientation angles of the chromophores. The models described above assume a completely rigid binding of each chromophore to its respective molecule; however, the possibility of limited chromophore rotational mobility within the embedding structure can easily be added by averaging the equations in column 3 in Fig. 2 over the range of physically allowed chromophore orientation angles. Complete averaging of each exact equation over the remaining orientation angles reduces it to the approximate equation in column 2, as expected.

## DISCUSSION

The applicability of nonradiative energy transfer rates between a donor-acceptor pair to the determination of their separation has long been recognized and used in numerous studies to evaluate distances at the molecular level (5, 16, 17). Thomas and co-workers have considered the energy transfer behavior between donors and acceptors freely diffusing in solution in the rapid diffusion limit, where the excited state lifetime of the donor is long enough to allow, on the average, many donor-acceptor collisions before deexcitation occurs. The rate of energy transfer in this case is directly related to the distance of closest approach between donor and acceptor (11) and was used in a number of studies to gain insight into the depths of binding sites and other structures below the surface of proteins and biological membranes (12-19). Although the long excited-state lifetime of the donor in these experiments may allow for complete rotational relaxation before transfer, it is clear (see Fig. 3) that such averaging of the relative dipole moment orientations is subject to limitations at small separations due to steric hindrance. This problem has been recognized before (11), but an analytical solution for the expected rate constant has been calculated for only one limiting case (18).

We now consider the differences between the quenching rates obtained by solving the exact equations and those obtained from the approximate equations (assuming complete angular randomization). The magnitude of the deviation between the two expressions for a given geometry is conveniently expressed as the ratio of the corresponding rate constants, and in general will depend on the chromophore orientation angles as well as on the sizes and shapes of the molecules represented in the geometry. Fig. 4 graphs this ratio versus  $\theta_{\mu 1}$  for the

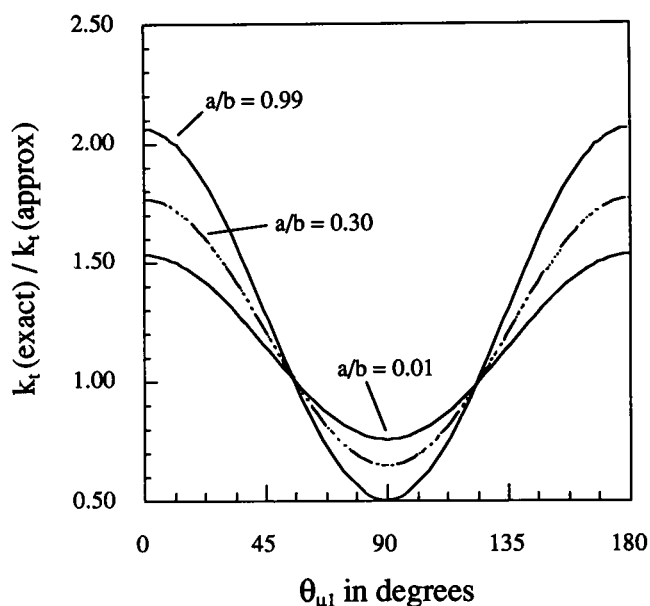


FIGURE 4. A comparison of the ratio of the exact and approximate equations for the energy transfer rate vs. dipole orientation angle  $\theta_{\mu 1}$  for several values of  $a/b$  for the vesicle geometry presented in row 2 in Fig. 2. Here  $a$  is the distance of closest approach of the donor and acceptor and  $b$  is the distance from the center of the vesicle to the acceptor. When the donors are much smaller than the vesicles ( $a/b \rightarrow 0$ ), this geometry becomes very similar to the planar geometry of Fig. 1. In both situations, the exact equation allows the transfer rate to vary by as much as a factor of two with chromophore orientation angle. When the donors are not much smaller than the vesicles ( $a/b \rightarrow 1$ ), the potential error is much greater. The exact and approximate equations give the same result for the quenching rate when  $\theta_{\mu 1} \approx 54.74^\circ$  and when  $\theta_{\mu 1} \approx 125.26^\circ$ , because for these angles  $\cos^2 \theta_{\mu 1} = 1/3$ , its averaged value.

geometry presented in Fig. 2, row 2 (involving donors trapped inside a vesicle) for several values of the parameter  $a/b$ , which is the ratio of the distance of closest approach to the distance from the donor to the center of the vesicle. The graph shows that the maximum possible error between the exact and approximate equations for this geometry occurs when the donor radius approaches the size of the vesicle radius ( $a/b \rightarrow 1$ ). For a geometry in which  $a/b \approx 1$ , the transfer rates calculated from the exact and approximate equations differ by more than a factor of two at the extreme values of  $\theta_{\mu 1} = 0^\circ$  or  $\theta_{\mu 1} = 180^\circ$ . For this value of  $a/b$  the exact equation also reveals a fourfold decrease in the quenching of an acceptor chromophore when its orientation relative to the perpendicular to the surface of the vesicle is changed from 0 to  $90^\circ$ . Potential error is minimized in this geometry when the trapped donors are much smaller than the vesicle ( $a/b \rightarrow 0$ ). In this limit the geometry becomes very similar to that in Fig. 1, involving a donor

embedded in a plane with freely diffusing acceptors. At the extreme values of  $\theta_{\mu 1} = 0^\circ$  or  $\theta_{\mu 1} = 180^\circ$  in such a geometry, the transfer rates calculated from the exact and approximate equations differ by 50%. The exact equation also reveals a factor of two decrease in the quenching of a donor chromophore when its orientation relative to the perpendicular to the surface of the vesicle (or plane) is changed from 0 to  $90^\circ$ .

For transfer when both dipoles are embedded in a planar membrane, row 4 in Fig. 2, the ratio of the deviation depends on the orientation of both dipoles relative to the plane. Fig. 5 graphs this ratio versus  $\theta_{\mu 1}$  for several fixed values of  $\theta_{\mu 2}$ . In this model the energy transfer rate is maximized when  $\theta_{\mu 1} = \theta_{\mu 2} = 90^\circ$ ; however, this transfer rate vanishes when one dipole is oriented at  $0^\circ$  or  $180^\circ$  and the other at  $90^\circ$ . In planar geometries, then, a dramatic dependence of the quenching rate on dipole orientation angles exists.

The relationships between transfer rates derived from the exact and approximate expressions for the geometries in rows 1 and 3 of Fig. 2 are more complicated than those described above. Each ratio involves dependences on  $r_1$ ,  $r_2$ ,  $\theta_{\mu 1}$ , and the appropriate offset variable ( $t$  or  $y$ ). As expected, in each of these geometries the approximate equations approach the exact equations when the parameters correspond to greater spherical symmetry

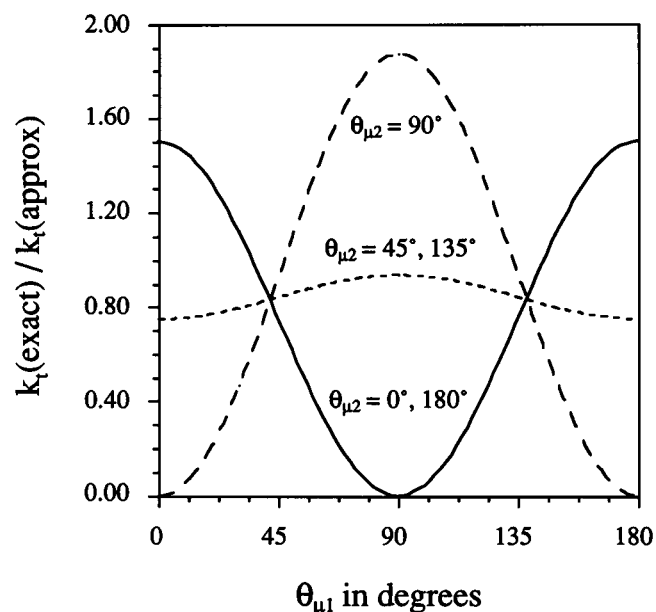


FIGURE 5. The dependence of the ratio of the exact and approximate energy transfer rates on dipole orientation angles for the geometry of row 4, Fig. 2. The transfer rate is maximal when  $\theta_{\mu 1} = \theta_{\mu 2} = 90^\circ$ , but this geometry also allows the transfer rate to go to zero for some combinations of orientation angles.

surrounding the donor and acceptor. In each geometry the situation corresponding to maximal error is when the radius of the freely diffusing sphere with the centered chromophore is much smaller than the radius of the embedding sphere of the other chromophore. In this situation both of these geometries approach that of Fig. 1, with its potential error of a factor of two in the transfer rate.

As discussed earlier, an important application of luminescence quenching by energy transfer in the rapid diffusion limit is to distance determination. For chromophores whose transition dipole directions are known, the exact equations are immediately useful for this purpose. For measurements involving a sample whose transition dipole orientation is not known, useful information is still available. These equations may be used to obtain information about the orientation angle itself, in addition to measuring a distance of interest. This can be done by testing the sample with two different probes with known characteristics in separate energy-transfer experiments. Each probe-sample pair is characterized by an equation relating the transfer rate to the desired distance and to the dipole orientation angle of the sample (more specifically, the square of the cosine of this orientation angle). With the measured  $k_t$  for each probe, two equations can be constructed relating the distance to the square of the cosine of the angle, thus presenting enough information to determine both quantities.

In cases where the chromophore orientation is unknown and two well characterized probes are not available, the exact equations can be used to set limits on the possible uncertainties in the distances being measured. For example, the approximate equations may be used to measure the distance of closest approach  $a$  between a donor and an acceptor (this quantity is given by  $a = r_1 + r_2 - t$  for the geometry of row 1 in Fig. 2, by  $a = r_1 + r_2$  in rows 3 and 4, and by  $a = r + h$  in Fig. 1). The exact equation shows that in a geometry in which the donor and acceptor are in freely diffusing spheres with one chromophore off-center, the approximation  $\kappa^2 = 2/3$  leads to errors of  $<4\%$  in the determined distance of closest approach, when the sphere with the off-center chromophore is the smaller sphere. For energy transfer in a geometry that involves a planar surface, the chromophore orientation can have a far greater impact. For a donor-acceptor pair embedded in a plane and a sphere, the fact that a twofold variation of  $k_t$  with dipole orientation angle is possible leads to a potential error of 26% in the distance of closest approach. When both donor and acceptor are embedded in the same plane, use of the approximate quenching rate formula may provide meaningless results due to the enormous variation of transfer rate with orientation angles. In some

applications of distance measurement, the errors given above may be acceptable, and the approximate equations will then provide an adequate estimate of the distance of closest approach. This distance, however, is often calculated for the further purpose of determining a distance characteristic to the sample, such as the depth of a chromophore beneath the surface of a protein or membrane. It should be noted that the relative error in that distance may be much larger than the relative error in the distance of closest approach, and in general it is not straightforward to decide in advance when the approximate equations will give adequate results.

## CONCLUSION

This study examines the effect that the orientation angles of chromophore transition dipole moments have on the rate of dipole-dipole energy transfer in the rapid diffusion limit. Explicit consideration of these angles in the derivation of the transfer rate equations yields expressions that show that in nonspherically symmetric geometries the transfer rate is strongly influenced by chromophore orientation. The exact equations presented here allow for more accurate distance determination for chromophores whose orientation is known and offer a means to determine both the orientation and position for some chromophores. When the orientation cannot be determined, these equations provide a means to calculate the error involved in using the approximate equations for distance measurement.

This research was supported by a Presidential Initiative Fund award to the University of Michigan from the W. K. Kellogg Foundation, by a grant from the Office of Naval Research, and by a grant from the National Institute on Aging (contract No. AG-09761). J. V. Mersol was supported by a training grant from the National Institute on Aging (contract No. T32AG-00114).

## REFERENCES

1. Eisinger, J. 1969. Intramolecular energy transfer in adrenocorticotropin. *Biochemistry*. 8:3902-3915.
2. Stryer, L., and R. P. Haugland. 1968. Energy transfer: a spectroscopic ruler. *Proc. Natl. Acad. Sci. USA*. 58:719-726.
3. Lin, T., and R. Dowben. 1983. Studies on the spatial arrangement of muscle thin filament protein using fluorescence energy transfer. *Proc. Natl. Acad. Sci. USA*. 258:5142-5150.
4. Steinberg, I. Z. 1971. Long-range nonradiative transfer of electronic excitation energy in proteins and polypeptides. *Annu. Rev. Biochem.* 40:83-115.
5. Stryer, L. 1978. Fluorescence energy transfer as a spectroscopic ruler. *Annu. Rev. Biochem.* 47:819-846.
6. Förster, T. 1948. Intermolecular energy migration and fluores-



- 
- cence. *Ann. Physik.* 2:55–75. (R. S. Knox, translator. University of Rochester, New York. 1984.)
7. Steinberg, I. Z. 1968. Nonradiative energy transfer in which rotary Brownian motion is frozen. *J. Chem. Phys.* 48:2411–2413.
  8. Hillel, Z., and C. Wu. 1976. Statistical interpretation of fluorescence energy transfer measurements in macromolecular systems. *Biochemistry.* 15:2105–2113.
  9. Dobryski, P. and M. Kochman. 1988. Fluorescence resonance energy transfer studies on the proximity between lysine 107 and cysteine 239 in rabbit muscle aldolase. *Biochim. Biophys. Acta.* 956:217–223.
  10. Dale, R. E., J. Eisinger, and W. E. Blumberg. 1979. The orientational freedom of molecular probes. The orientation factor in intramolecular energy transfer. *Biophys. J.* 26:161–193.
  11. Thomas, D. D., W. F. Carlsen, and L. Stryer. 1978. Fluorescence energy transfer in the rapid-diffusion limit. *Proc. Natl. Acad. Sci. USA.* 75:5746–5750.
  12. Yeh, S. M., and C. F. Meares. 1980. Characterization of transferin metal-binding sites by diffusion enhanced energy transfer. *Biochemistry.* 19:5057–5062.
  13. Wensel, T. G., C. H. Chang, and C. F. Meares. 1985. Diffusion-enhanced lanthanide energy-transfer study of DNA-bound cobalt(III) bleomycins: comparisons of accessibility and electrostatic potential with DNA complexes of ethidium and acridine orange. *Biochemistry.* 24:3060–3069.
  14. Mersol, J. V., D. G. Steel, and A. Gafni. 1991. Quenching of tryptophan phosphorescence in *Escherichia coli* alkaline phosphatase by long-range transfer mechanisms to external agents in the rapid diffusion limit. *Biochemistry.* 30:668–675.
  15. Stryer, L., D. D. Thomas, and C. F. Meares. 1982. Diffusion-enhanced fluorescence energy transfer. *Annu. Rev. Biophys. Bioeng.* 11:203–222.
  16. Leder, R. O., S. L. Helgerson, and D. D. Thomas. 1989. The transverse location of the retinal chromophore in the purple membrane by diffusion-enhanced energy transfer. *J. Mol. Biol.* 209:683–701.
  17. Thomas, D. D., and L. Stryer. 1982. Transverse location of the retinal chromophore of rhodopsin in rod outer segment disc membranes. *J. Mol. Biol.* 154:145–157.
  18. Kouyama, T., K. Kinoshita, Jr., and A. Ikegami. 1983. Fluorescence energy transfer studies of transmembrane location of retinal in purple membranes. *J. Mol. Biol.* 165 91–107
  19. Meares, C. F., and L. S. Rice. 1981. Diffusion-enhanced energy transfer shows accessibility of ribonucleic acid polymerase inhibitor binding sites. *Biochemistry.* 20:610–617.